JOURNAL OF ADVANCED DIELECTRICS
Vol. 4, No. 3 (2014) 1450021 (5 pages)

DOI: 10.1142/S2010135X14500210

World Scientific
www.worldscientific.com

Ultralow frequency dielectric dispersion in PZT + PFS ferroelectric ceramic

Andrzej Osak
Institute of Physics, Cracow University of Technology
ul. Podchorążych 1, Kraków 30-084, Poland
puosak@cyfronet.pl

Received 2 April 2014; Revised 17 July 2014; Accepted 18 July 2014; Published 8 August 2014

The depolarization decaying currents were measured for the PZT compound with morphotropic composition modified by the $Fe_{1/3}Sb_{2/3}$ cations, i.e., $Pb[(Fe_{1/3}Sb_{2/3})_xTi_yZr_z]O_3$ with $x + y + z = 1$, $x = 0.1$, $y = 0.44$ (morphotropic boundary) and $y = 0.47$. The measurements were performed at room temperature and a few temperatures above (up to 473 K), as well as at a few lower temperatures (down to 77 K). The samples were poling at fields 0.02 kV/cm and 0.2 kV/cm at higher and lower temperatures, respectively. In the high temperature range, the time dependence depolarization current follows the fractional power law with two different exponents ($n < 1$ and $m > 1$), while in the low temperature range with a single exponent (n). The appropriate procedure has been used to transform the results obtained in the time domain into the frequency domain in order to calculate real and imaginary parts of the dielectric permittivity in the frequency range $5 \times 10^{-5} - 0.1$ Hz. The possible dielectric relaxation mechanisms have been discussed.

Keywords: Ferroelectric ceramics; PZT-PFS; depolarization currents; dielectric permittivity.

1. Introduction

The dielectric relaxation at low and ultralow frequencies has been widely investigated in many materials,[1,2] including ferroelectric perovskite crystals[3,4] and ceramic structures.[5,6] Usually, the measurements are carried out down to 10^{-3}–10^{-5} Hz and various experimental equipments have been developed for this purpose.[2,7–9] Investigation of the low-frequency dielectric relaxation in the oxide octahedron-type ferroelectric with perovskite PMN,[3,10] PMNT,[11] tungsten bronze-type PBN[12] and $NaBiTiO_3$[13] structures are of considerable interest because of possibility of their technical application as actuators, pyroelectric detectors and transducers.

Earlier studies of the $Fe_{1/3}Sb_{2/3}$ ions-modulated PZT show its good dielectric, pyroelectric and electromechanical properties.[14,15] Studies of low-frequency dielectric dispersion can explain ageing effect, domain wall motion as well dipoles, ions and electrons dynamics. Relaxation behavior of ferroelectric ceramics depends strongly on poling field and temperature. The studies on the relaxation properties of the PZT + PFS were partly presented.[16] Present studies are concerned with measurements and analysis of the relaxation properties of the $Pb[(Fe_{1/3}Sb_{2/3})_xTi_yZr_z]O_3$ with $x + y + z = 1$, $x = 0.1$, $y = 0.44$ and 0.47 compositions in the range of low poling fields (linear range).

2. Dielectric Relaxation

Dielectric relaxation phenomena usually are investigated in the transient or frequency domains. In the transient response we use the relaxation function $F(t)$, which describe polarization decay after an electric field is switched off or the response function $f(t)$ which describes the evolution of polarization after an electric field is applied. In the frequency domain the relaxation behavior are described by dielectric susceptibility $\chi(\omega)$ or permittivity $\varepsilon(\omega)$. In the case linear dielectric

$$f(t) = -\frac{dF(t)}{dt}.$$

The simplest of dielectric response is represented by Debye exponential function

$$\exp\left(-\frac{t}{\tau}\right)$$

with single relaxation time τ. The Debye model was extended by postulate superposition of the Debye response with distribution $w(t)$ relaxation times.

$$f(t) = \int w(t) \exp\left(-\frac{t}{\tau}\right) d\tau. \quad (1)$$

The experimental results explained the following response functions: stretched exponential Kohlrausch–Williams–Waltts $\exp[-(\frac{t}{\tau})^n]$, fractional power law Curie–von Schwiedler t^{-n} and Jonsher two fractional power type $[(\omega_p t)^{-n} + (\omega_p t)^{-m}]$ where $\tau = \tau_p^{-1}$ define a crossover regime between two different relaxation one for short time $f(t) \sim (\omega_p t)^{-1}$ and second for long time $f(t) \sim (\omega_p t)^{-m}$. Dissado and Hill have formulated the theory of dielectric relaxation considering the dynamics of dipoles and charge carriers in cluster model.[17,18]

Dissado–Hill response function in the asymptotic short and long limit time give also fractional power low as the Jonsher expression but for time ω_p^{-1} one observe exponential behavior. Lately, the theory of dielectric relaxation was developed on the basis probabilistic and stochastic theory.[19] In the frequency domain a number of empirical expressions have been proposed to describe particular types of dielectric dispersion. The well-known frequency responses there are Debye, Cole-Cole, Davison Cole, Williams–Watts, and other.[2]

3. Transient Current Method

The low-frequency dielectric measurements are usually performed in the time domain, while high frequency ones are performed in the frequency domain. The dc transient current method is suitable for the measurements in the frequency region lower than mHz. The measurement of the transient depolarization currents are frequently used to eliminate contribution dc conductivity in the imaginary part of dielectric permittivity. The relation between the relaxation currents and dielectric permittivity $\varepsilon(\omega)$ is given by the Fourier transformation

$$\varepsilon(\omega) = \int_0^\infty \frac{J(t)}{V_0 C_0} \mathrm{e}^{-i\omega t} dt, \tag{2}$$

where V_0 is the voltage applied to a dielectric and C_0 condenser geometric capacitance. Relaxation process in the low-frequency range has generally a wide distribution of the relaxation times. Therefore, Fourier transformation of the observed transient current has to be carried out over a wide frequency range (4 or 5) decades. The procedures for numerical Fourier transformation suitable for a wide frequency range were developed by many authors. See Refs. 20–22 for more details.

4. Experimental Procedure

Prior we have searched for the range of the linear dependence depolarization currents on the poling field. From the preliminary measurements it was found that in the high temperature range the linear dependence fulfilled (valid) up to 0.02 kV/cm whereas for lower temperatures up to 0.2 kV/cm.

The samples were subjected to an electric poling field and the decaying current was measured at two applied fields, namely 0.02 kV/cm and 0.2 kV/cm in the high and low temperature range, respectively. After poling, the applied field was removed and the sample was short-circuited via a current measuring Keithley electrometer, type 6517A, until the reversal decaying depolarization current had disappeared. The measurements of depolarization currents have allowed to eliminate leakage currents. All measurements were carried out in the ferroelectric phase. In the case of low temperature measurements down to 77 K, a Linkam stage was used. The experimental results are collected using a computer program. In all experiments, the disc-like samples with thickness of 0.5 mm, surface 0.36 cm^2 and with silver electrodes were used.

5. Results

The decaying isothermal depolarization currents $J_d(t)$ for samples with $y = 0.44$ are shown in Figs. 1(a) and 1(b) at high and low temperature ranges, respectively. Similarly, the depolarization currents for sample with $y = 0.47$ are shown in Figs. 2(a) and 2(b).

The results shown in Figs. 1(a) and 2(a) indicate that the time-dependent depolarization currents at high temperatures may be represented, in the log–log scale, by two straight lines, one at initial times with the slope n and the second at final times with the slope m, according to formula[2]

$$I_d(t) = \frac{A}{(\frac{t}{\tau_0})^n + (\frac{t}{\tau_0})^m}, \tag{3}$$

where A is a constant and τ_0 is the parameter defined by frequency ω_0 at which the loss peak appears, i.e., $\omega_0 = \frac{1}{\tau_0}$.

Depolarization currents $J_d(t)$, measured for both samples at low temperatures, show not any crossover regions and may be described by a single straight line with slope n (see Figs. 1(b) and 2(b)). The small values depolarization current for depolarization time longer than $5 \cdot 10^4$ s have not allowed to detect crossover regions.

The Fourier transformation was used to transform measured depolarization current into frequency dependence dielectric permittivity $\varepsilon(\omega)$. Numerical evaluation of the Fourier transformation was based on a simple summation

$$\varepsilon(\omega) = \Delta t \sum_{n=0}^{N} \exp(-i\omega\Delta t) \cdot J_d(n\Delta t). \tag{4}$$

The time intervals Δt and number of terms N was chosen in such way to eliminate aliasing and truncation errors. The measurements of the depolarization currents were carried out over a long time period such as $5 \cdot 10^4$ s. The numerical integration was performed in six intervals according to six time range Δt used (from $\Delta t = 1$ to $\Delta t = 1000$ s).

The low-frequency dependencies of the imaginary part of the dielectric permittivity $\varepsilon''(\omega)$ are presented in Figs. 3(a) and 3(b) for samples with $y = 0.44$ and 0.47, respectively. As can be seen, the high-temperature data are characterized by a maximum that shifts towards higher frequencies with increasing temperature. On the other hand, the low-temperature data show a monotonic decrease with increasing frequency. The real part of the dielectric permittivity $\varepsilon'(\omega)$ for both samples is shown in Figs. 4(a) and 4(b). Comparison of Figs. 3 and 4 indicate that both real and imaginary parts of the dielectric permittivity are higher for sample with $y = 0.44$ (the morphotropic composition) than for sample with $y = 0.47$.

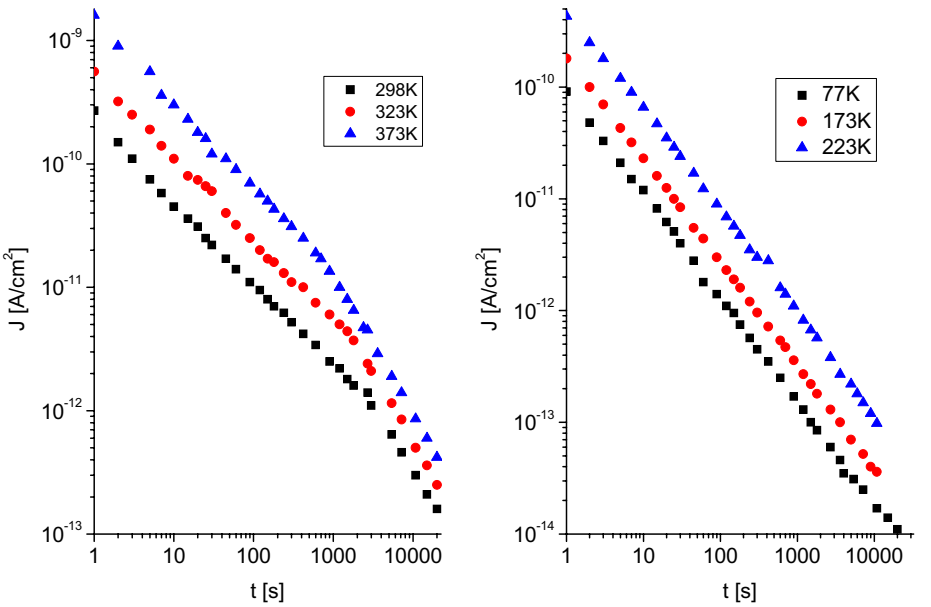

Fig. 1. Time dependence of decaying depolarization currents for sample with $y = 0.44$ measured at selected high (a) and low temperatures (b). Poling field for (a) is 0.02 kV/cm and for (b) is 0.2 kV/cm.

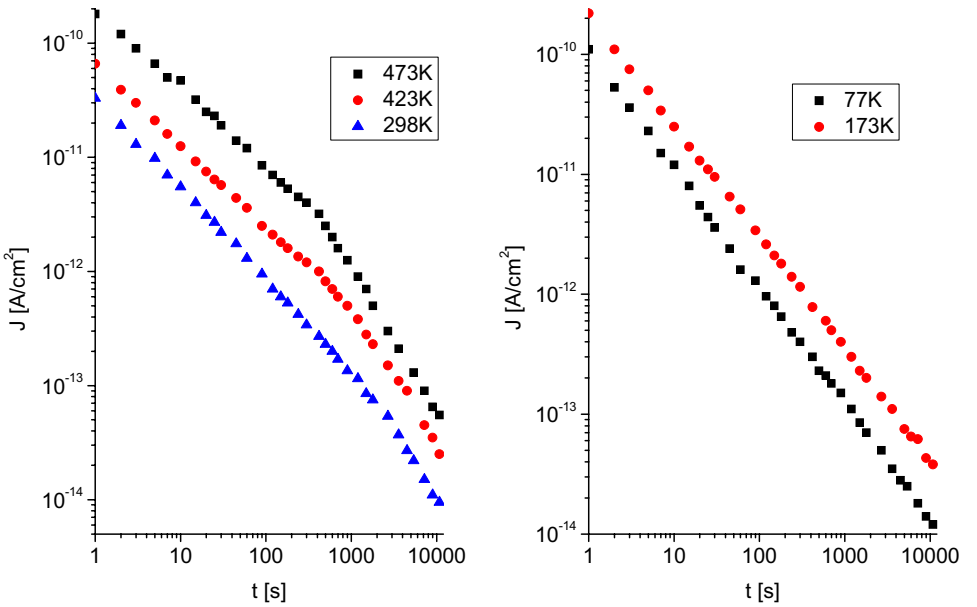

Fig. 2. Time dependence of decaying depolarization currents for sample with $y = 0.47$ measured at selected high (a) and low temperatures (b). Poling field for (a) is 0.02 kV/cm and for (b) is 0.2 kV/cm.

6. Discussion

(1) Many investigations have shown that the low-frequency dielectric relaxation in perovskite ferroelectrics is caused by different crystal lattice defects. In the lead zirconate titanate compound (PZT), the most probable defect species are lead and oxygen vacancies, and random or near random distribution of Ti and Zr ions. Doping PZT with Fe and Sb ions introduces new defects. The Fe^{3+} ions are known to substitute Ti^{4+} or Zr^{4+} ions,[23] whereas, as may be inferred from Ref. 24, the Sb^{3+} (90 pm) ions may be substituted for Pb^{2+} ions introducing oxygen vacancies, while smaller Sb^{5+} (60 pm) ions may be incorporated in Zr(Ti) sublattice providing free electrons.

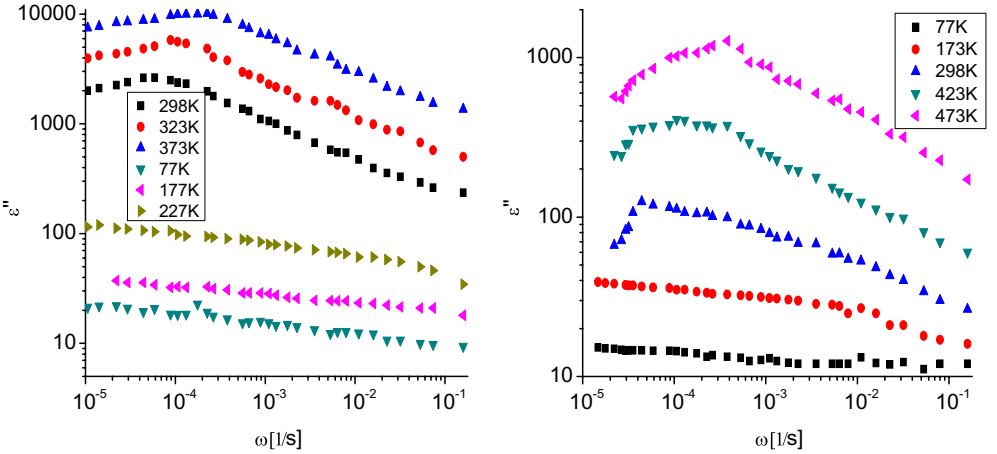

Fig. 3. Low-frequency dependence of the imaginary part of the dielectric permittivity for samples with $y = 0.44$ (a) and $y = 0.47$ (b) at selected temperatures.

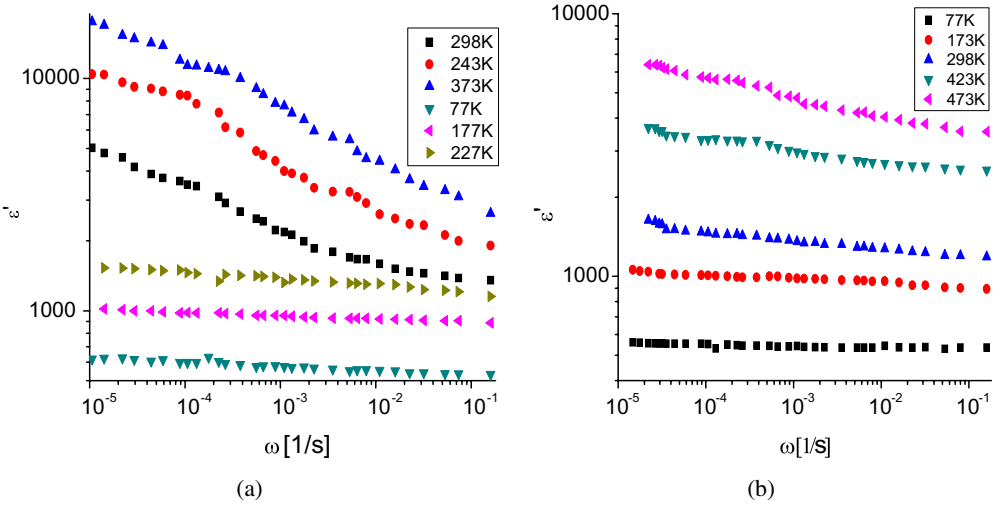

Fig. 4. Low-frequency dependence of the real part of the dielectric permittivity for samples with $y = 0.44$ (a) and $y = 0.47$ (b) at selected temperatures.

In the case of PZT with Fe^{3+} ions, three Fe_{TiZr}–V_O complex defects can be formed depending on whether an oxygen atom is removed or not. The energy barrier for reorientation of defected complexes depends on the position of oxygen vacancies with respect to iron atom.[23] In the tetragonal phase of the PZT, there are two types of oxygen atoms, the oxygen atoms bonded to two Ti atoms in ab-planes [O(2)] and the oxygen atoms in O–Ti–O chains in c-direction [O(1)]. Therefore, we may expect three kinds of defected complexes.

The observed in higher temperatures, for both samples, the Debye-type relaxation maxima (see Figs. 3(a) and 3(b)) can be attributed to the reorientation of defected complex formed with a smaller energy barrier and created by oxygen vacancies situated in ab plane of the perovskite structure.

(2) In a crystal lattice, different existing defects may be single or may be aggregated into clusters (microregions) with various size and composition. Such a defected complex disturbs the charge distribution into the crystal lattice, causes the local deformation and interacts with a neighboring cluster. The short-range intercluster interaction between different clusters (e.g., cluster composed of the Ti^{4+}, Zr^{4+} and Fe^{3+} cations — oxygen coordinated octahedrons) controls the kinetics of the slow relaxation polarization and depolarization currents. A nanoscale cluster has the dipole moment that may thermally fluctuate between different equivalent directions. A re-arrangement of the large cluster dipole in poling fields leads to slow relaxation polarization. The observed at initial time, comparatively faster polarization decay is due to the kinetics

of the rearrangements of intracluster dipole and ions or electrons displacement.[17,18]

(3) Earlier XRD studies[25] have shown a coexistence of the rhombohedral and tetragonal ferroelectric phases for sample with $y = 0.44$, characterized by the morphotropic phase boundary (MPB), as well as for sample with $y = 0.47$ that is far from MPB. The ratio of the rhombohedral to the tetragonal phases in sample with $y = 0.44$ is equal to 38/62 that is much greater than 2/98 for sample with $y = 0.47$.

In multiaxial ferroelectric phases, the polar vector may rotate between equivalent crystallographic orientations. In the samples studied, polarization may have a maximum number of equivalent orientations equal to 6 for tetragonal and 8 for rhombohedral phases. However, as suggested in Ref. 12, the potential barriers along $\langle 111 \rangle$ directions, representing crystalline anisotropy of the rhombohedral phase, are shallow and, for this reason, may give a significant contribution to the overall sample polarization. The enhanced polarization in sample with $y = 0.44$ may be due to a significant amount of the rhombohedral phase in this sample, as compared to sample with $y = 0.47$.

7. Conclusion

The broad relaxation maximum of $\varepsilon''(\omega)$ suggests contributions of all discussed relaxation mechanisms in the total sample polarization.

However, taking into account the temperature-activated dependence of $\varepsilon''(\omega)$ and the value of the activation energy (0.2 eV), approximately equal to energy reorientation of Fe_{TiZr}–V_O defect dipoles in the perovskite structures (calculated theoretically in Ref. 23), we suggest that, in the range of low poling fields (0.02 kV/cm), the dominant relaxation mechanism is reorientation of these defect dipoles.

Acknowledgments

The author is grateful to J. Cisowski and W. Osak for suggestions and helpful discussion.

References

[1]C. J. F. Bötlcher and P. Bordewijk, *Theory of Electric Polarization*, 2nd edn., Chapters VIII and IX (Elsevier, Amsterdam, 1978).
[2]A. K. Jonscher, *Dielectric Relaxation in Solids* (Chelsea Dielectric Press, London, 1983).
[3]E. V. Colla, E. Yu. Koroleva, N. M. Okuneva and S. B. Vakhushev, Low-frequency dielectric response of $PbMg_{1/3}Nb_{2/3}O_3$, *J. Phys. Condens. Matter* **4**, 3671 (1992).
[4]Y. Park, Low-frequency-dispersion of $Pb(Fe_{1/2}Nb_{1/2})O_3$ single crystal in the region of its paraelectric ferroelectric phase transition, *Solid State Commun.* **113**, 379 (2000).
[5]H. Neuman and G. Arlt, Transient polarization currents and degradation affects in $BaTiO_3$ and $SrTiO_3$ ceramics, *Proc. 6 IEEE Inst. Bethlem.* (1986), pp. 357–360.
[6]F. Chu, H.-T. Sun, L. Y. Zhang and X. Yao, Temperature dependence of ultra-low-frequency dielectric relaxation of barium-titanate ceramics, *J. Am. Ceram. Soc.* **75**, 2939 (1992).
[7]M. A. Perez Jubindo, M. J. Tello and J. Fernandez, A new method for measuring the ferroelectric behavior of crystals at low frequencies, *J. Phys. D Appl. Phys.* **14**, 2305 (1981).
[8]R. Gerson, Dielectric properties of lead titanate zirconate of very low frequencies, *J. Appl. Phys.* **31**, 1615 (1960).
[9]Z. Liangyixg, Y. Xi, H. A. McKinstry and L. E. Cross, Quasi-static capacitance and ultra slow-relaxation of linear and non-linear dielectrics, *Ferroelectrics* **49**, 75 (1983).
[10]T. A. Nealon, Low-frequency dielectric response in PMN-type ceramics, *Ferroelectrics* **76**, 377 (1987).
[11]A. A. Bokov and Z. G. Ye, Low frequency dielectric spectroscopy of the relaxor-ferroelectric $Pb(Mg_{1/3}Nb_{2/3})O_3$-$PbTiO_3$, *Phys. Rev. B* **65**, 144112 (2002).
[12]R. Guo, A. S. Bhalla, C. A. Randall and L. E. Cross, Dielectric and pyroelectric properties of the morphotropic phase boundary lead barium niobate (PBN) single crystals at low temperature (10-300 K), *J. Appl. Phys.* **67**, 6405 (1990).
[13]J. Suchanicz, The low frequency dielectric relaxation Na $BiTiO_3$ ceramics, *Mat. Sci. Eng. B* **55**, 114 (1998).
[14]I. Jankowska-Sumara, W. Śmiga and R. Bujakiewicz-Korońska, The piezoelectric effect in $Pb[(Fe_{1/3}Sb_{2/3})_xTi_yZr_z]O_3$ ceramics, *Phase Transit.* **81**, 1107 (2008).
[15]I. Jankowska-Sumara, Dielectric and pyroelectric properties of $Pb[(Fe_{1/3}Sb_{2/3})_xTi_yZr_z]O_3$, *Ferroelectrics* **345**, 115 (2006).
[16]A. Osak, Relaxation currents in morphotropic region of $Pb[(Fe_{1/3}Sb_{2/3})_xTi_yZr_z]O_3$ ferroelectric ceramic, *Phase Transit.* **86**, 926 (2013).
[17]L. A. Dissado and R. M. Hill, Anomalus low-frequency dispersion, *J. Chem. Soc.* **80**, 291 (1984).
[18]L. A. Dissado and R. M. Hill, Dielectric anomalous behaviour of materials undergoing dipole alignment transitions, *Phil. Mag. B* **41**, 625 (1980).
[19]A. K. Jonsher, A. Jurlewicz and K. Weron, Stochastic schemes of dielectric relaxation in correlated-cluster systems, *Contemp. Phys.* **44**, 329 (2009).
[20]H. Blick, R. Gröves, P. W. Lord and S. M. Walker, Treatment of data in step-response dielectric relaxation measurement, *J. Chem. Soc. Faraday Trans. 2* **68**, 1890 (1972).
[21]S. Takeishi and S. Mashimo, Dielectric relaxation measurements in the ultralow-frequency region, *Rev. Sci. Instrum.* **63**, 1155 (1982).
[22]F. J. Mopsik, The transformation of time-domain relaxation data into the frequency-domain, *IEEE Trans. Electr. Insulat.* **EI-20**, 957 (1985).
[23]P. Marton and C. Elsässer, Switching of a substitutional-iron/oxygen vacancy defect complex in ferroelectric $PbTiO_3$ from first principles, *Phys. Rev. B* **83**, 020106(R) (2011).
[24]J. Nowotny and J. Rekas, *Defect Structure and Electrical Properties of Barium Titanate*, ed. J. Nowotny, Electronic Ceramic Materials (Trans Tech Publications, Zürich, 1992), pp. 1–44.
[25]A. Osak, W. S. Ptak, W. Osak and C. Strzałkowska, Dielectric and electric properties of policrystaline $Pb[(Fe_{1/3}Sb_{2/3})_xTi_yZr_z]O_3$, *Ferroelectrics* **154**, 247 (1994).